IFSCC 2025 full paper (IFSCC2025-606)

"Study on the effect of rice fermentation filtrate on cellular energy metabolism and mitochondrial function"

Zuo Jinhui[1,*], Wang Hua[1], Hu Yawen[1], Guo Miao[1], Yang Fan[1]

1 Mageline Biology Tech Co., Ltd., wuhan, China;

1. Introduction

Rice fermentation filtrate contains a variety of active components, including amino acids, sugars, organic acids, nucleic acids and peptides [1]. Our previous research demonstrated that rice fermentation filtrate obtained by fermenting rice with *Saccharomyces veronae*, offers significant skincare benefits such as enhanced hydration, improved elasticity, and reduced wrinkles [2]. Furthermore, it is rich in α-ketoglutaric acid (α-KG) and succinic acid, both of which are involved in the tricarboxylic acid (TCA) cycle, crucial for cellular energy production [2-4]. However, the specific mechanism of action of rice fermentation filtrate on skin cell energy metabolism and mitophagy is unclear.

Research shows that cellular energy metabolism involves key targets such as ATP, NAD+,, PGC-1α, AMPKα, SIRT1, SIRT3, SIRT6, LC3-I, LC3-II, and p62. ATP is the main energy source for the cell, essential for metabolism and cell division [5]. NAD+ plays critical roles in metabolic pathways, ATP synthesis, energy metabolism, DNA repair, and aging, and is often used as a marker of cell health and aging status [6]. PGC-1α regulates mitochondrial biogenesis [7], while AMPKα helps balance energy by promoting energy production and inhibiting energy consumption [8]. SIRT1, SIRT3, and SIRT6 are NAD+-dependent deacetylases that regulate cellular stress response, mitochondrial function, and DNA repair [9-11]. LC3-I and LC3-II are autophagy markers, with LC3-II indicating active autophagosome formation [12]. p62 is a protein involved in autophagy that links damaged proteins to autophagic degradation [13]. Together, these targets coordinate energy metabolism, mitochondrial function, and cellular stress responses.

To further investigate its mechanism, we performed several assays, including ATP, and NAD+ measurements using Biochemical kits, mitochondrial morphology analysis with Mito-Tracker Green fluorescence. in addition, qPCR and Western blotting to assess key mitochondrial and autophagy-related targets such as PGC-1α, AMPKα, SIRT1, SIRT3, SIRT6, LC3-I, LC3-II, and p62.

2. Materials and Methods

2.1 Materials

C1 - Internal use

Lyophilized Rice Fermentation Filtrate (RFF, Laboratory-made), Human Dermal Fibroblasts (HDF, ELK Biotechnology), PBS Solution (AS1044, ASPEN), Physiological Saline (AS1087, ASPEN), BCA Protein Assay Kit (AS1086, ASPEN), ATP Assay Kit (S0026, Biyuntian), NAD+ Assay Kit (S0175, Biyuntian), Mito-Tracker Green (C1048, Biyuntian), Hoechst33342 (B8040, Solarbio), TRIpure Total RNA Extraction Reagent (EP013, ELK Biotechnology), Chloroform (10006818, Sinopharm Chemical Reagent), Isopropanol (80109218, Sinopharm Chemical Reagent), RNase-Free Water (Custom), 1st Strand cDNA Synthesis Super Mix (EQ031, ELK Biotechnology), SYBR Green PCR SuperMix (EQ001, ELK Biotechnology), PGC-1α, SIRT1, SIRT3, SIRT6 (ELK Biotechnology)， SDS-PAGE Gel Preparation Kit (AS1012, ASPEN), RIPA Lysis Buffer (AS1004, ASPEN), BCA Protein Assay Kit (AS1086, ASPEN), ECL Detection Reagent (AS1059, ASPEN), PVDF Membranes (IPVH00010, Millipore), Antibodies (GAPDH (ab181602, abcam), p62 (ab109012, abcam), AMPKα (#2532, CST), LC3 (#12741, CST).

2.2 Methods

2.2.1 ATP and NAD+ measurement

(1) Sample Preparation: Cells were extracted by adding 200 μL of extraction solution per 1×10^6 cells, followed by centrifugation to collect the supernatant. The sample groups were as follows: A: HDF; B: HDF + UVA (10 J/cm²); C: HDF + UVA (10 J/cm²) + Lyophilized RFF (62.5 μg/mL); D: HDF + UVA (10 J/cm²) + Lyophilized RFF (125 μg/mL); E: HDF + UVA (10 J/cm²) + Lyophilized RFF (250 μg/mL); F: HDF + UVA + Lyophilized RFF (500 μg/mL).

(2) ATP, NAD+ Measurement: The enhanced ATP Assay Kit was used to measure ATP level by luciferase luminescence assay. A standard curve was prepared with known ATP concentrations. The enhanced NAD+ Assay Kit was used to measure NAD+ levels. Samples were treated with ethanol dehydrogenase, followed by the addition of a color reagent, then incubated for 10 minutes at 37°C, and absorbance was measured at 450 nm to quantify ATP, NAD+ levels.

2.2.2 Mitochondrial morphology Analysis

Mito-Tracker Green was used to stain live cell mitochondria, independent of mitochondrial membrane potential. The procedure involved removing the culture medium and washing the cells with PBS or serum-free medium three times. Mito-Tracker Green was then diluted at a ratio of 1:5000 in PBS or serum-free medium and incubated with the cells at 37°C for 30 minutes, protected from light. After incubation, the cells were washed three times with PBS or serum-free medium. Hoechst33342 was added for nuclear staining, and the cells were incubated for 30 minutes at 25℃. The cells were washed again and immediately observed under a fluorescence microscope.

2.2.3 qPCR Analysis

To assess the expression of genes related to mitochondrial energy metabolism (PGC-1α, SIRT1, SIRT3 and SIRT6), quantitative PCR (qPCR) was performed. RNA was extracted by aspirating the culture medium, washing the cells with pre-chilled PBS, and then adding TRIpure reagent followed by chloroform. After a 5-minute incubation on ice, the mixture was centrifuged at 10,000 g for 10 minutes at 4°C, and the upper aqueous phase was collected. For cDNA synthesis, 2 μg of RNA was mixed with 1st Strand cDNA Synthesis Super Mix and

C1 - Internal use

incubated at 25°C for 5 minutes, 42°C for 30 minutes, and 85°C for 5 minutes. The qPCR was carried out using the SYBR Green PCR SuperMix on a QuantStudio 6 Flex System with each sample run in triplicates. The cycling conditions were as follows: 95°C for 30 seconds, followed by 40 cycles of 95°C for 10 seconds, 58°C for 30 seconds, and 72°C for 30 seconds. A melting curve analysis was performed to verify the specificity of amplification, with primer sequences provided in **Table 1**.

Table 1. The information of primer sequences

Name		primer sequence（5'-3'）
GAPDH	sense	CATCATCCCTGCCTCTACTGG
	antisense	GTGGGTGTCGCTGTTGAAGTC
PGC-1α	sense	GATGTGAACGACTTGGATACAGAC
	antisense	GTCTAGTGTCTCTGTGAGGACTGC
SIRT-1	sense	TACTTCGCAACTATACCCAGAAC
	antisense	CCTGATTAAAAATATCTCCTCGTAC
SIRT-3	sense	TCACTTTGGCCAAGGAGCT
	antisense	CTCTCAAGCCCATCGATGTTC
SIRT-6	sense	CAAGTTCGACACCACCTTTGAG

2.2.4 Western blot analysis

Western blotting was used to analyze proteins related to mitochondrial energy metabolism and autophagy, including LC3-I, LC3-II, p62, and AMPKα.The protein extraction procedure involved washing cells with PBS and lysing them in RIPA buffer supplemented with protease inhibitors. After incubating on ice for 30 minutes, the mixture was centrifuged at 12,000 g for 5 minutes at 4°C, and the supernatant was collected. Protein concentration was then measured using the BCA Protein Assay Kit. For SDS-PAGE and Western blotting, protein samples were mixed with 5× sample buffer, heated at 95°C for 5 minutes, and separated by SDS-PAGE at 80V for the stacking gel and 120V for the separating gel. Proteins were transferred to PVDF membranes using a semi-dry blotting apparatus at 300 mA. Membranes were blocked with 5% non-fat milk in TBS-T for 1 hour, incubated with primary antibodies overnight at 4°C, washed with TBS-T, and incubated with secondary antibodies for 1 hour. Bands were visualized using ECL detection reagent and analyzed with AlphaEaseFC software.

3. Results

3.1 Enhancement of ATP and NAD+ Levels by RFF

The experimental results from **Figure 1** show that UVA exposure significantly decreases ATP and NAD+ production in HDF cells. With the addition of different concentrations of Rice Fermentation Filtrate (RFF) significantly increased ATP levels. The highest ATP levels were observed in the 250 μg/mL RFF-treated group (E), which showed a 2.5-fold increase compared

to the UVA-exposed group (B). Similarly, NAD+ levels were elevated in the 250 μg/mL RFF group (E), suggesting enhanced mitochondrial function in response to RFF treatment.

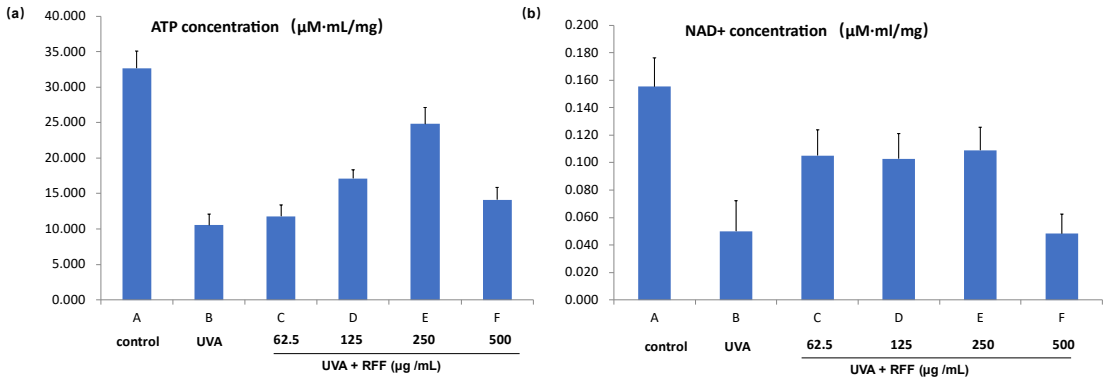

Figure 1. Effects of RFF on ATP and NAD+ production. (a) Effect of RFF on ATP production in HDF; (b) Effect of RFF on NAD+ production in HDF. A: HDF; B: HDF + UVA (10 J/cm²); C: HDF + UVA (10 J/cm²) + Lyophilized RFF (62.5 μg/mL); D: HDF + UVA (10 J/cm²) + Lyophilized RFF (125 μg/mL); E: HDF + UVA (10 J/cm²) + Lyophilized RFF (250 μg/mL); F: HDF + UVA + Lyophilized RFF (500 μg/mL)

3.2 Mitochondrial Morphology Test

Mitochondrial morphology was assessed using Mito-Tracker Green staining, and the results showed that under UVA exposure, mitochondria were damaged, appearing spherical or short rod-like. Compared to the UVA-exposed group, RFF-treated cells exhibited a more elongated and interconnected mitochondrial network (**Figure 2**). These findings suggest that RFF can protect the normal morphology of mitochondria of fibroblasts under UV stress, potentially enhancing mitochondrial dynamics and contributing to improved cellular energy metabolism.

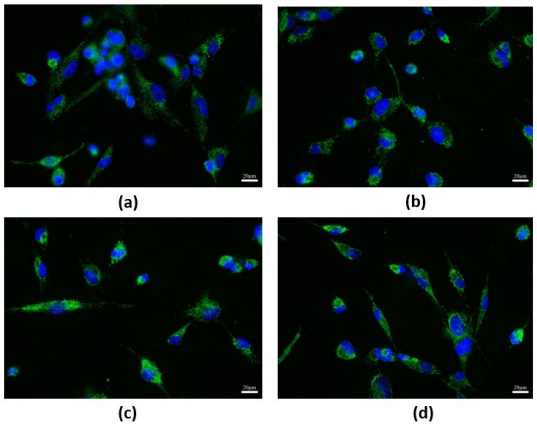

Figure 2. Mitochondrial morphology (Mito-Tracker Green staining). (a) no treat HDF; (b) HDF + UVA ; (c) HDF + UVA+ Lyophilized RFF (125 μg/mL); (d) HDF + UVA+ Lyophilized RFF (500 μg/mL).

3.3 Quantitative PCR (qPCR) Analysis

C1 - Internal use

As shown in **Figure 3**, qPCR results demonstrated that RFF treatment significantly upregulated the expression of mitochondrial biogenesis markers, including PGC-1α, SIRT1, SIRT3, and SIRT6. Specifically, when RFF was added at a concentration of 500 μg/mL, there was a significant increase in the expression of PGC-1α, SIRT1, SIRT3, and SIRT6 in Human Dermal Fibroblasts (HDF). At a concentration of 250 μg/mL, SIRT1, SIRT3, and SIRT6 gene expression showed a significant increase, while no significant effect was observed on PGC-1α expression. No significant changes in gene expression were noted at lower concentrations of RFF. These results suggest a potential role of RFF in promoting mitochondrial function and biogenesis.

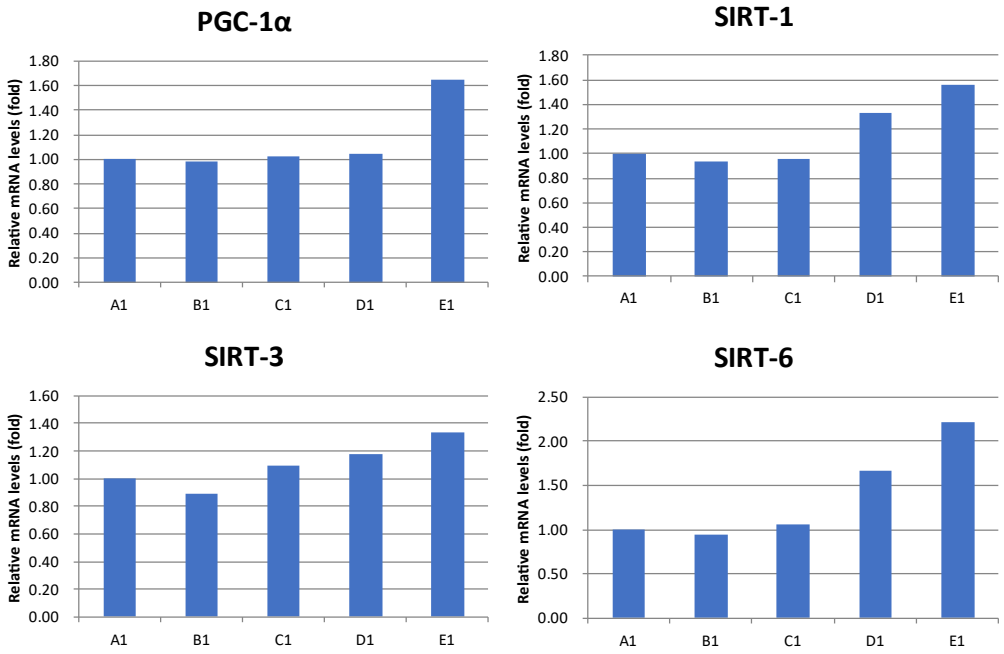

Figure 3. qPCR analysis for PGC-1α, SIRT1, SIRT-3 and SIRT-6 gene expression in HDF treated with different concentrations of RFF. A1: HDF; B1: HDF + Lyophilized RFF (62.5 μg/mL); C1: HDF + Lyophilized RFF (125 μg/mL); D1: HDF + Lyophilized RFF (250 μg/mL); and E1: HDF + Lyophilized RFF (500 μg/mL)

3.4 Western Blot Analysis

Based on the Western blot results shown in **Figure 4**, the data indicates that RFF at lower concentrations (62.5, 125, and 250 μg/mL) did not significantly affect the expression of LC3-I, LC3-II, p62, or AMPKα proteins in HDF cells. However, when the concentration of RFF reached 500 μg/mL, there was no significant change in the expression of p62 or AMPKα. Notably, the expression of both LC3-I and LC3-II was significantly elevated, and the LC3-I/LC3-II ratio was also significantly increased. Since the conversion of LC3-I to LC3-II is a marker for autophagosome formation, these results suggest that RFF at 500 μg/mL concentration can effectively promote autophagy.

C1 - Internal use

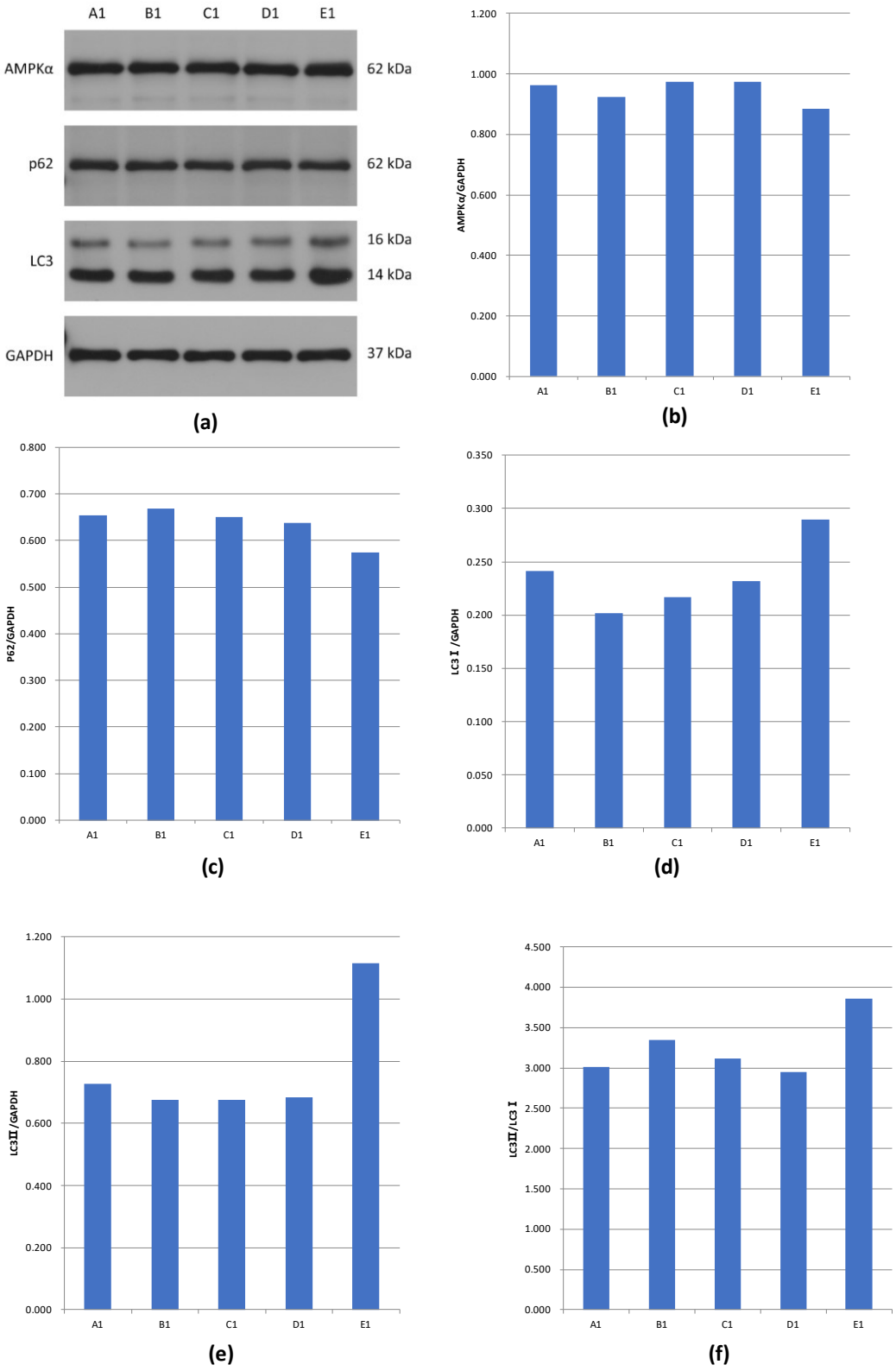

Figure 4. Western blot (WB) analysis of LC3-I, LC3-II, p62, and AMPKα protein levels in in Human Dermal Fibroblasts treated with different concentrations of Rice fermentation filtrate. (a) Proteins on PVDF membranes were targeted with anti- LC3-I, anti- LC3-II, anti-p62, anti-

p-AMPKα and anti-GAPDH antibodies. GAPDH was used as the loading control. (b) Protein levels of AMPKα were normalized to those of GAPDH. (c) Protein levels of p62 were normalized to those of GAPDH. (d) Protein levels of LC3-I, were normalized to those of GAPDH. (e) Protein levels of LC3-II, were normalized to those of GAPDH. (f) Protein levels of LC3-II/ LC3-I. A1: HDF; B1: HDF + Lyophilized RFF (62.5 μg/mL); C1: HDF + Lyophilized RFF (125 μg/mL); D1: HDF + Lyophilized RFF (250 μg/mL); and E1: HDF + Lyophilized RFF (500 μg/mL).

4. Discussion

In our experiments, we tested the effects of RFF on various cellular energy metabolism and autophagy-related targets, including ATP, NAD+, PGC-1α, AMPKα, SIRT1, SIRT3, SIRT6, LC3-I, LC3-II, and p62. The effects of these targets are summarized in **Table 2** [5-14].

Table 2. The function of targets related to cellular energy metabolism and autophagy.

Target	Function
ATP	Serves as the primary energy source for the cell, involved in various biological processes, including metabolism and cell division. ATP production is closely linked to mitochondrial function.
NAD+	NAD+ is an essential coenzyme in redox reactions, involved in metabolic pathways, including glycolysis, fatty acid β-oxidation, and the electron transport chain. Regulation of NAD+ levels is crucial for cellular energy metabolism.
PGC-1α	A master regulator of mitochondrial biogenesis, PGC-1α promotes mitochondrial DNA replication and the expression of oxidative phosphorylation genes, enhancing cellular energy generation.
AMPKα	AMPK senses cellular energy status and regulates energy balance by inhibiting energy-consuming processes and promoting energy production, including activating PGC-1α to enhance mitochondrial biogenesis.
SIRT1	SIRT1 regulates gene expression through NAD+-dependent deacetylation, controlling metabolism, aging, and oxidative stress responses, and influences mitochondrial function by activating PGC-1α.
SIRT3	SIRT3 deacetylates key enzymes in the mitochondria, boosting antioxidant responses, regulating the electron transport chain, and ATP synthesis to maintain mitochondrial health.
SIRT6	SIRT6 is involved in DNA repair, aging, and metabolic regulation, promoting antioxidant responses and regulating mitochondrial function, though its direct interaction with PGC-1α is limited.
LC3-I	LC3-I is an important marker in the autophagy process, involved in the formation of autophagosomes. LC3-I converts to LC3-II and associates with the autophagosome membrane to help clear cellular waste.
LC3-II	LC3-II is the active form in autophagy, associating with the autophagosome membrane, playing a critical role in encapsulating and transporting autophagic material for degradation.

C1 - Internal use

p62	p62 is an autophagy adaptor protein that recognizes and binds ubiquitinated proteins, participating in both autophagy and mitophagy.

The experimental results showed that RFF significantly promoted the expression of ATP and NAD+ in HDF under UVA exposure, and improved mitochondrial morphology, restoring it to a more elongated and interconnected network. The qPCR results revealed that higher concentrations of RFF (250 μg/mL or 500 μg/mL) significantly increased the gene expression of PGC-1α, SIRT1, SIRT-3, and SIRT-6 in HDF. However, the Western blot analysis showed that RFF only significantly increased the expression of LC3-I, LC3-II, and the LC3-II/LC3-I ratio at a concentration of 500 μg/mL, with no significant effect on p62 and AMPKα. This suggested that RFF may have promoted autophagy by enhancing the expression of LC3-I and facilitating its conversion into LC3-II [12, 15].

Based on the combined results from biochemical tests, qPCR, and Western blot tests, we hypothesize that RFF may promote mitochondrial biogenesis by enhancing the expression of SIRT3 in HDF, which in turn stimulates mitochondrial ATP synthase. Furthermore, RFF might increase SIRT1 expression, which subsequently promotes PGC-1α expression, leading to enhanced mitochondrial biogenesis and restoration of mitochondrial morphology. Additionally, RFF can promote the conversion of LC3-I to LC3-II, thus activating mitophagy, as shown in **Figure 5**.

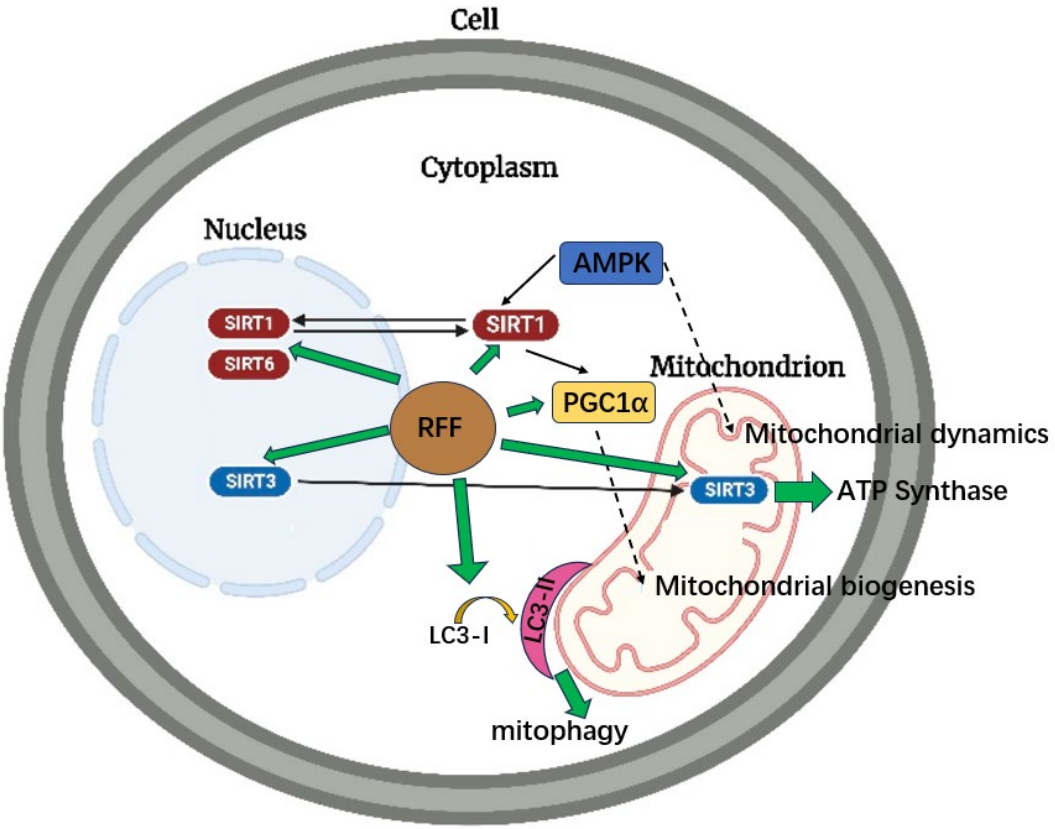

Figure 5. Schematic diagram of RFF mechanism of action [14-16].

However, there are some limitations in this experiment. For instance, we did not precisely determine the cellular location where RFF acts on these targets, and it remains unclear whether its effects occur in the nucleus, cytoplasm, or mitochondria. Moreover, the

concentrations of RFF tested in the experiment require further optimization to establish a clearer dose-response relationship. In future studies, we will further explore which specific active components of RFF are responsible for activating the energy metabolism and autophagy-related targets in cells.

5. Conclusion

In conclusion, this study demonstrates that rice fermentation filtrate (RFF) has a significant impact on cellular energy metabolism and autophagy in HDF, especially under oxidative stress induced by UVA exposure. The results indicate that RFF enhances mitochondrial function, as evidenced by increased ATP, and NAD+ levels, and improves mitochondrial morphology, restoring it to a healthier, interconnected state. Furthermore, RFF treatment upregulated key mitochondrial biogenesis markers such as PGC-1α, SIRT1, SIRT3, and SIRT6. At higher concentrations, RFF also promoted the conversion of LC3-I to LC3-II, suggesting an activation of autophagy. These findings suggest that RFF could play a crucial role in mitochondrial biogenesis and mitophagy, potentially offering new insights into skin cell rejuvenation and anti-aging treatments. However, further research is needed to expore the specific active components of RFF and their exact mechanisms in regulating these processes.

References

[1] Yang, F., Hu, Y., Wu, M., Guo, M., & Wang, H. (2025). Biologically Active Components and Skincare Benefits of Rice Fermentation Products: A Review. Cosmetics, 12(1), 29.

[2] Yang, F., Zhou, Z., Guo, M., & Zhou, Z. (2022). The study of skin hydration, anti-wrinkles function improvement of anti-aging cream with alpha-ketoglutarate. *Journal of Cosmetic Dermatology*, *21*(4), 1736-1743.

[3] Polito, M. P., Romaldini, A., Rinaldo, S., & Enzo, E. (2024). Coordinating energy metabolism and signaling pathways in epithelial self-renewal and differentiation. *Biology Direct*, *19*(1), 63.

[4] Papurina, T., Barsukov, O., Zabuga, O., Krasnienkov, D., & Denis, E. (2023). Effects of succinic acid on dermal fibroblasts during cultivation under extremely hypoxic conditions. *Biochemistry and Biophysics Reports*, *33*, 101429.

[5] Mason, E. F., & Rathmell, J. C. (2011). Cell metabolism: an essential link between cell growth and apoptosis. *Biochimica et Biophysica Acta (BBA)-Molecular Cell Research*, *1813*(4), 645-654.

[6] Ying, W. (2006). NAD+ and NADH in cellular functions and cell death. *Front Biosci*, *11*(1), 3129-3148.

[7] Wenz, T. (2013). Regulation of mitochondrial biogenesis and PGC-1α under cellular stress. Mitochondrion, 13(2), 134-142.

[8] Ke, R., Xu, Q., Li, C., Luo, L., & Huang, D. (2018). Mechanisms of AMPK in the maintenance of ATP balance during energy metabolism. Cell biology international, 42(4), 384-392.

[9] Sosnowska, B., Mazidi, M., Penson, P., Gluba-Brzózka, A., Rysz, J., & Banach, M. (2017). The sirtuin family members SIRT1, SIRT3 and SIRT6: Their role in vascular biology and atherogenesis. Atherosclerosis, 265, 275-282.

C1 - Internal use

[10] Yang, T., & Sauve, A. A. (2006). NAD metabolism and sirtuins: metabolic regulation of protein deacetylation in stress and toxicity. *The AAPS journal*, *8*, E632-E643.
[11] Sauve, A. A., & Youn, D. Y. (2012). Sirtuins: NAD+-dependent deacetylase mechanism and regulation. *Current opinion in chemical biology*, *16*(5-6), 535-543.
[12] Tanida, I., Ueno, T., & Kominami, E. (2008). LC3 and Autophagy. Autophagosome and phagosome, 77-88.
[13] Ichimura, Y., & Komatsu, M. (2010, December). Selective degradation of p62 by autophagy. In *Seminars in immunopathology* (Vol. 32, pp. 431-436). Springer-Verlag.
[14] Clark, A. J., & Parikh, S. M. (2021). Targeting energy pathways in kidney disease: the roles of sirtuins, AMPK, and PGC1α. *Kidney international*, *99*(4), 828-840.
[15] Liu, H., Dai, C., Fan, Y., Guo, B., Ren, K., Sun, T., & Wang, W. (2017). From autophagy to mitophagy: the roles of P62 in neurodegenerative diseases. Journal of bioenergetics and biomembranes, 49, 413-422.
[16] Hamaidi, I., & Kim, S. (2022). Sirtuins are crucial regulators of T cell metabolism and functions. *Experimental & molecular medicine*, *54*(3), 207-215.

C1 - Internal use